

Gravity Scaling of Pool Boiling Heat Transfer

Jungho KIM¹, Rishi RAJ² and John McQUILLEN³

Abstract

Recent developments in our understanding of gravity effects on pool boiling heat transfer are discussed. An experimental apparatus using a fast response microheater array was used to obtain data throughout the continuously varying gravity levels during the transition from hypergravity (1.8 G) to low-G (~0.01 G) using low-G aircraft. A similar heater was used to obtain boiling data in the very quiet microgravity environment of the International Space Station as part of the Microheater Array Boiling Experiment. This data has allowed the development of a unified model to predict the boiling heat transfer at any gravity level if the heat transfer at a reference gravity level (e.g., earth gravity) is known. The model is first discussed and validated against experimental data from the International Space Station, then used to explain previous low-G data from other groups.

1. Introduction

Much confusion exists regarding the effect of gravity on pool boiling heat transfer despite the efforts of many researchers and experiments performed over the past five decades. The primary cause of this confusion is the assumption that a single power law can describe how heat transfer varies with gravity. Correlations for heat flux in the nucleate boiling regime are often in the form of a power law:

$$q''_{boiling} = f(c_g, c_p, h_{lv}, p, \alpha, \mu, \rho_l, \rho_v, \sigma, \Delta T_{sub}) * \Delta T_w \left(\frac{a}{g}\right)^m \quad (1)$$

As an example, the Rohsenow correlation¹⁾ given by

$$\frac{q''}{\mu_l h_{lv} \left[\frac{\sigma}{g(\rho_l - \rho_v)} \right]^{1/2}} = \left(\frac{1}{C_{sf}} \right)^{1/r} \text{Pr}_l^{-s/r} \left\{ \frac{c_{pl} [T_w - T_{sat}(P_l)]}{h_{lv}} \right\}^{1/r} \quad (2)$$

suggests the gravity dependence in nucleate boiling is described using a power law coefficient $m=1/2$. Similarly, the critical heat flux (CHF) correlation of Kutateladze²⁾ given by

$$q''_{max} = 0.131 \rho_v h_{lv} \left[\frac{\sigma(\rho_l - \rho_v) g}{\rho_v^2} \right]^{1/4} \quad (3)$$

suggests $m=1/4$.

For constant fluid properties, fluid subcooling (ΔT_{sub}), and wall superheat, the logarithm of Eq. 1 yields

$$\log(q''_{boiling}) = \left[k + n \log(\Delta T_w) \right] + m \log\left(\frac{a}{g}\right) = C + m \log\left(\frac{a}{g}\right) \quad (4)$$

If this power form is assumed, a linear variation in $\log(q'')$ vs. $\log(a/g)$ with slope m would be expected for a given superheat. Furthermore, changes in wall superheat and gas concentration should affect the intercept C only, and not affect the slope m .

To verify the power law and determine the constants C and m ,

high quality data over a *continuous range* of gravity levels is desired. Earth gravity data, of course, can readily be obtained. Platforms commonly used to study low gravity effects such as drop towers, parabolic aircraft, sounding rockets, and spacecraft can be used to provide data at near zero-G environments. However, partial gravity data between earth gravity and zero-G is quite rare.

Fortunately, parabolic aircraft do traverse a continuous range of gravity levels as the aircraft transitions from the hypergravity regime to the low-G regime as shown in **Fig. 1**. If this platform is coupled with a test apparatus with a heater whose frequency response is much faster than the boiling process, and if the boiling process is in turn fast enough to respond to the changing gravity level such that the boiling can be thought of as quasi-steady state, the transitions between hypergravity to low-G can be used to obtain data over a continuous range of gravity levels.³⁾

The objective of this paper is to summarize the results of a series of experiments in which a fast response microheater array is used to obtain pool boiling data in the variable gravity environment provided by low-G aircraft as well as the microgravity environment of the International Space Station. It is demonstrated that a single power law of the form given by Eqs. 1 and 4 *cannot* be used to describe the effects of gravity on pool boiling heat transfer due to fundamental changes in the boiling behavior from a buoyancy dominated regime (bubbles depart the surface periodically) to a surface tension dominated regime (non-departing primary bubble covering the heater). Methods to determine the heat transfer at any gravity level given the heat transfer at a reference gravity level are then discussed and validated.

1 Corresponding author, Dept. of Mechanical Engineering, University of Maryland, College Park, MD 20742 USA (kimjh@umd.edu)

2 Currently with the Dept. of Mechanical Engineering, Massachusetts Institute of Technology, Cambridge, MA 02139 USA

3 NASA Glenn research Center, 21000 Brookpark Road, Cleveland, OH 44125 USA

Nomenclature

a	acceleration (m/s^2)
BDB	buoyancy dominated boiling
c_g	gas concentration (ppm)
CHF	critical heat flux
g	acceleration due to gravity (m/s^2)
H	Henry's constant (mole/mole-Pa)
K_{jump}	scaling factor for jump in q''
L_h	width of square heater (m)
L_c	capillary length (m), $\sqrt{\sigma / a(\rho_l - \rho_v)}$
Ma	Marangoni number
m	power law coefficient for gravity, $q'' \propto g^m$
ONB	onset of nucleate boiling
P, p	pressure (Pa)
q''	heat flux (W/cm^2)
R'	ratio of characteristic length to capillary length
RMS	root mean square
SDB	surface tension dominated boiling
T	temperature ($^{\circ}\text{C}$)
T^*	non-dimensional temperature, $(T_w - T_{ONB}) / (T_{CHF} - T_{ONB})$
w	weighting factor
Greek	
α	thermal diffusivity (m^2/s)
μ	dynamic viscosity ($\text{Pa}\cdot\text{s}$)
ρ	density (kg/m^3)
σ	surface tension (N/m)
Subscripts	
app	apparent
$bulk$	bulk liquid
c	condensation
$depart$	departure
e	evaporation
ref	reference condition
sat	saturation
sub	subcooling
$tran$	transition
t	total
v	vapor
w	wall

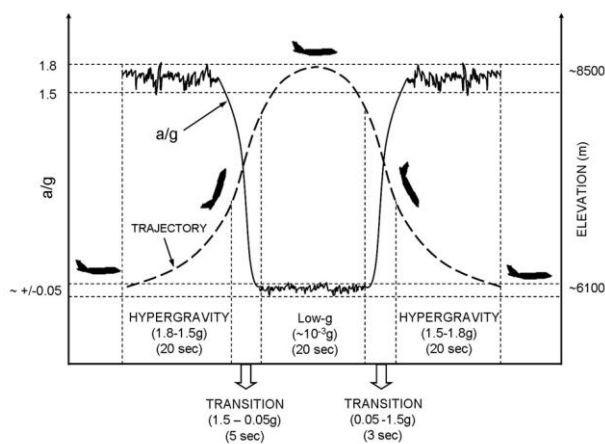


Fig. 1 Schematic of one parabola on the ESA Airbus A300 low-G aircraft: trajectory and acceleration level.

2. Experimental Apparatus

2.1 Microheater array

A microheater array consisting of 96 platinum resistance heaters deposited in a 10x10 configuration onto a quartz substrate was used to measure the heat transfer distribution (**Fig. 2**). Each heater in the array was nominally $0.7 \times 0.7 \text{ mm}^2$ in size. Power was transferred via gold power leads $1 \text{ }\mu\text{m}$ thick. Individual heaters had a nominal resistance of $250 \text{ }\Omega$ and a temperature coefficient of resistance (TCR) of $0.0022^{\circ}\text{C}^{-1}$. The heater array could provide a maximum heat flux of 220 W/cm^2 locally. The reader is referred to Rule and Kim⁴⁾ for the details of the heater construction. The heater temperature was kept constant using a bank of feedback circuits similar to those used in constant temperature hot-wire anemometry. The power, and thus the heat flux, required to maintain these heaters at the desired temperature were obtained by sampling the voltages across the heaters. The frequency response for the heaters and feedback circuits was very high (15 kHz) since the thermal lag was negligible due to the constant temperature boundary condition. Side view and bottom view images of the boiling process were captured to visualize the phenomena occurring near the heater surface and correlated with the heat transfer data.

2.2 Low-G aircraft flight apparatus

Three liters of 98.9% n-perfluorohexane, a straight chain isomer of C_6F_{14} ($T_{sat}=56^{\circ}\text{C}$ at 1 atm), was used as the test fluid. This isomer is also the principal constituent of FC-72, an electronic cooling fluid manufactured by 3M and used in many past experiments. The test rack contained a sealed boiling chamber with fluid at a pressure of 1 atm, the microheater array, the electronic feedback circuits, two video cameras, a computer, an accelerometer (Entran EGCS3), a pressure sensor (PDCR 130/W), some thermocouples and RTDs for the bulk liquid and air-jet temperature measurements, and a LCD display.

Backside cooling of the microheater array was required to minimize the lateral conduction and to prevent individual heaters from shutting off at low heat transfer levels. Air was

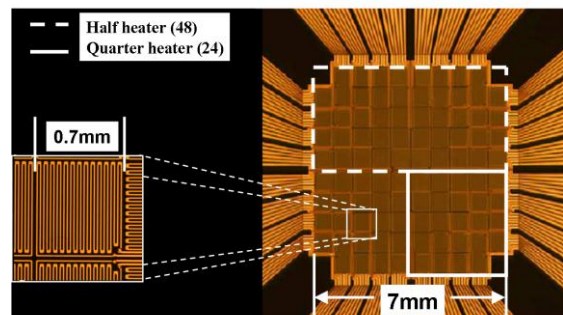


Fig. 2 Platinum resistance heater array, each element = $0.7 \times 0.7 \text{ mm}^2$.

forced through a 1.6 mm diameter nozzle placed 10 mm from the backside of the heater. The cooling air flow was maintained by a compressed air bottle with pressure regulation nominally set at 150 kPa. The ambient pressure inside the aircraft was measured to be 83 kPa and the air-jet temperature varied between 22°C and 24°C.

2.3 ISS flight apparatus

The Boiling eXperiment Facility (BXF)⁵⁾ utilizes the ISS as a platform to obtain pool boiling heat transfer data at very low gravity conditions. BXF incorporates two experiments within a single apparatus: the Microheater Array Boiling Experiment (MABE) and the Nucleate Pool Boiling Experiment (NPBX). Only the MABE results are reported here. The layout of BXF is shown in Fig. 3. Its principle elements are the Containment Vessel (CV) and Avionics Box (AB) that were mounted inside the Microgravity Science Glovebox (MSG) on the ISS. Local acceleration measurements were provided by a Space Acceleration Measurement System sensor head mounted in the MSG. BXF contained approximately 4 l of n-perfluorohexane.

3. Results and Discussion

As mentioned in Section 1, the transition from hypergravity (>1.5G) to low-G (<0.05G) and vice versa occurs over a period of about three to five seconds on the low-G aircraft (Fig. 1). In order to study heat transfer during this transition, the heat flux must be in quasi-steady state at any given gravity level. A plot of the boiling heat flux versus acceleration during the transition from hypergravity to low-G and vice versa at two superheats ($\Delta T_w=9^\circ\text{C}$ and $\Delta T_w=44^\circ\text{C}$) is shown on Fig. 4³⁾. Ideally, if the flow field and heat transfer profiles have sufficient time to achieve steady state at each acceleration level, there should be no difference between the two curves. However, a hysteresis effect in the heat flux curve is present at the lower superheat ($\Delta T_w=9^\circ\text{C}$) (Fig. 4, top). This was observed whenever the

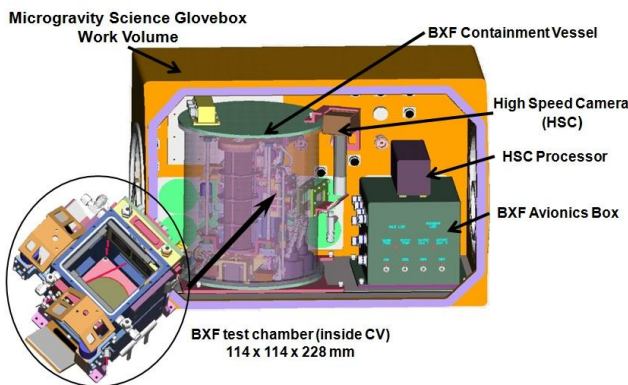


Fig 3 BXF mounted in MSG with transparent CV (Inset: view of the boiling chamber housing the two microheater arrays).

superheat was not sufficient to initiate nucleation, and heat transfer was primarily by natural convection. As the gravity changes, time is required for the flow field and heat transfer profiles to develop and achieve steady state. Before the transition from high-G to low-G, the natural convection flow field was fully developed. During the transition from high-G to low-G, the flow field required more time to achieve steady state than was available, resulting in higher heat transfer than the expected quasi-steady value. Similarly, during the transition from low-G to high-G, the heat transfer was lower than the expected quasi-steady value. However, at $\Delta T_w=44^\circ\text{C}$ (Fig. 4, bottom), the heat transfer is independent of the direction of transition. At this temperature, the majority of heat transfer is due to bubble growth and bubble departure. Since bubble departure frequencies can be as high as 30-40 Hz at normal gravity, the heat transfer during the transitions when boiling occurs are quasi-steady. The 15 kHz response of the heater and feedback circuit coupled with the data acquisition frequency of 100 Hz rule out any chances of discrepancies due to data collection. In the results to follow, only data where the heat transfer was quasi-steady were considered.

3.1 BDB and SDB Boiling Regimes

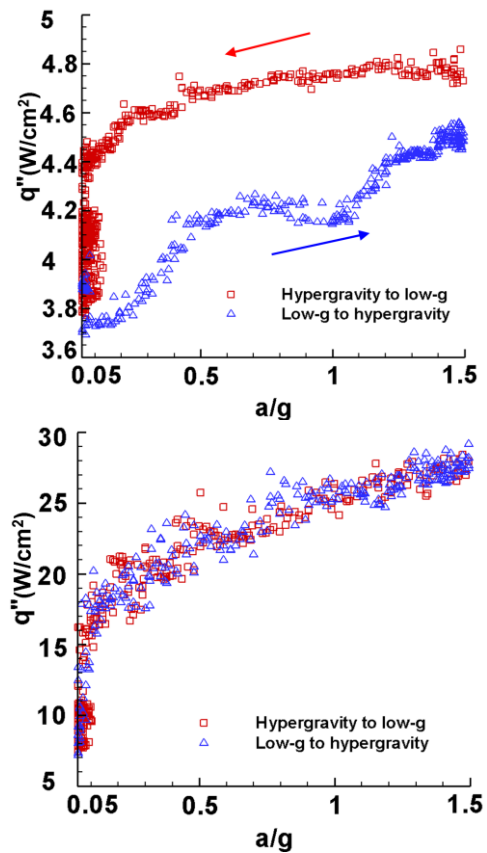


Fig. 4 Heat flux vs. acceleration during transition for $\Delta T_w=9^\circ\text{C}$ (top) and $\Delta T_w=44^\circ\text{C}$ (bottom), full heater ($7.0 \times 7.0 \text{ mm}^2$).

To verify the power law dependence assumed in Eqs. (1) and (4), the boiling heat flux data was binned based on gravity level into equal intervals of 0.005G. The average heat flux within each bin was assigned to the midpoint acceleration of each bin. Data points corresponding to negative acceleration values (g-jitter) were rejected. An example of the data is shown in **Fig. 5** where the data are plotted on log-log coordinates. A sharp change in heat flux is observed in this case between 0.1G-0.2G indicating a distinct change in the heat transfer mechanism. *This rules out the possibility of using a single power law to describe gravity dependence as per Eqs. (1) and (4).*

The heat transfer regime that occurs above the transition acceleration will hereafter be referred to as the BDB (Buoyancy Dominated Boiling) regime, while the regime below this transition will be referred to as the SDB (Surface tension Dominated Boiling) regime. The BDB regime was observed at higher accelerations and/or with larger heaters. A normal ebullition cycle consisting of bubble growth and departure from the surface was observed. The heat flux was independent of heater size in the BDB regime. The SDB regime was characterized by the formation of a non-departing coalesced bubble on the heater, and occurred at lower acceleration levels and/or with smaller heaters.

3.2 Gravity Scaling Methodology

A method of scaling the effects of gravity between the boiling heat transfer at a given reference gravity level to the heat transfer at another gravity level is desired. For example, suppose the heat transfer at Martian gravity, Lunar gravity, or the microgravity within spacecraft is desired based on the heat transfer measured in normal earth gravity. A generalization of the boiling behavior is schematically shown on **Fig. 6**. Assume

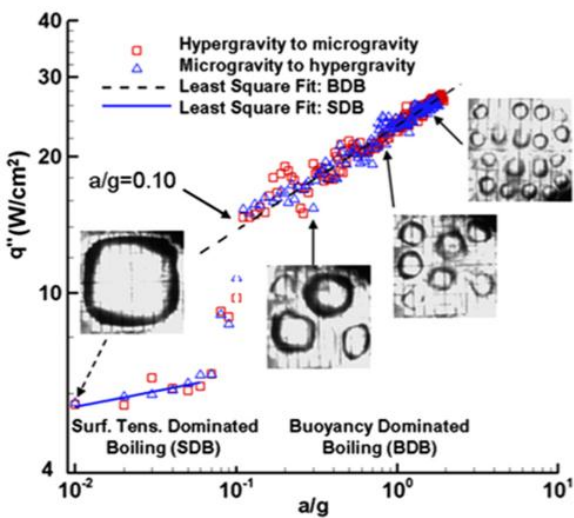


Fig. 5 Plot of heat flux vs. acceleration for high gas case ($c_g \sim 1216\text{ppm}$), full heater ($7.0 \times 7.0 \text{ mm}^2$), at $\Delta T_w = 44^\circ\text{C}$, with superimposed bottom view images at 0.01g, 0.3g, 0.85g and 1.68g.

we know the heat transfer at a reference point (point 1) and we desire to find the heat transfer in the microgravity of space (point 4'). The following information is required: the slope in the BDB regime (m_{BDB}), the location of a/g where the regime changes from BDB to SDB (a_{tran}/g), the magnitude of the change in heat flux as the boiling behavior changes from BDB to SDB ($\Delta q''$), and the slope in the SDB regime (m_{SDB}). The methodology by which each of these quantities is determined is discussed below.

3.2.1 Slope in BDB regime (m_{BDB})

The heat flux in the BDB regime was found to be independent of heater size, but dependent on the wall superheat. The power law coefficient (m_{BDB} : slope of the line 1-2-3 in **Fig. 6**) that accounts for gravity effects on heat flux in the BDB regime was found to be given by the following function⁶⁾:

$$m_{BDB} = \frac{0.65T^*}{1 + 1.6T^*} \text{ where } T^* = \frac{T_w - T_{ONB}}{T_{CHF} - T_{ONB}} \quad (5)$$

T^* is a non-dimensional temperature defined in the nucleate boiling regime whose value ranges from 0 at the onset of nucleate boiling (ONB) to 1 at critical heat flux (CHF), resulting in a power law coefficient m_{BDB} that varies from 0 at ONB to 0.25 at CHF. Based on this variation in m_{BDB} , a gravity scaling parameter for heat flux within the BDB regime is given by:

$$q''_{a2} = q''_{a1} \left(\frac{a_2}{a_1} \right)^{m_{BDB}} \quad (6)$$

This scaling parameter was shown to accurately predict pool boiling heat flux in the BDB regime at any gravity level (a_2) if the data under similar experimental conditions were available at any other reference acceleration level (a_1).

3.2.2 Acceleration at which transition between BDB to SDB occurs (a_{tran})

If the acceleration was reduced below a threshold acceleration (a_{tran}), a transition (3 and 3' in **Fig. 6**) occurred

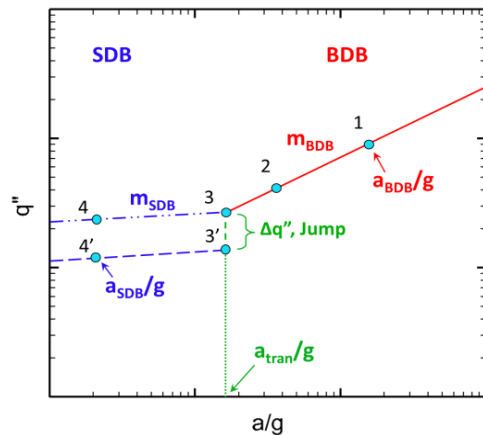


Fig. 6 Schematic of heat flux vs. acceleration at a given wall superheat.

wherein a change in the slope (3-4) or a change in the slope coupled with a jump in heat flux (3-3'-4') was observed. The criterion for determining the acceleration at which the transition from BDB to SDB occurs was found to be ^{6,7)}:

$$\frac{L_h}{L_c} = \frac{L_h}{\sqrt{\frac{\sigma}{(\rho_l - \rho_v) a_{tran}}}} = 2.1 \Rightarrow a_{tran} = \frac{4.41\sigma}{L_h^2(\rho_l - \rho_v)} \quad (7)$$

The transition acceleration is observed to increase with decreasing heater size. Boiling on large heaters can be in the BDB regime if the gravity is low enough. Similarly, boiling on small heaters can be dominated by surface tension at high gravity levels.

3.2.3 Change in heat flux at a_{trans} ($\Delta q''$)

The sharp jump in heat flux at the transition acceleration (q_3''/q_3'' in Fig. 6) was attributed to the tendency of the non-departing bubble in SDB to increase in size such that the condensation heat transfer at the bubble cap was balanced by the evaporation heat transfer at the bubble base given the absence of bubble departure. Decreases in subcooling and heater size, and increases in dissolved gas concentration were observed to increase the size of the jump. The jump in heat flux at transition was found to be a function of the Marangoni number Ma as follows⁵⁾:

$$K_{jump} = \frac{q_3''}{q_3''} = 1 - e^{-C \cdot Ma} \quad (8)$$

where

$$Ma = -\frac{d\sigma}{dT} \frac{\Delta T_{sub,app} L_h}{\mu \alpha} \quad (9)$$

and $C = \text{constant}$, $\Delta T_{sub,app} = T_{sat@p_v} - T_{bulk}$ and $p_v = p_t - p_g = p_t - c_g / H(T)$. The apparent subcooling, $\Delta T_{sub,app}$, was based on the vapor pressure (p_v), not on the total pressure (p_t), in order to capture the effect of dissolved gas concentration on the jump.

A single non-dimensional number, Ma , was used as the scaling parameter since it contains the other two parameters affecting the jump, namely the subcooling and the heater size. Marangoni number (Ma) is a non-dimensional quantity that has often been used to quantify microgravity heat transfer. Since the gradient of surface tension with temperature is negative for common fluids, Ma as defined above, is always positive; hence, the value of K_{jump} varies from 0 to 1. It was determined that $C = 8.3 \times 10^{-6}$ for FC-72⁶⁾. Large jumps ($K_{jump} \rightarrow 0$) to low heat transfer levels in the SDB regime were observed small Marangoni numbers ($Ma < 10^4$) while negligible jumps ($K_{jump} \rightarrow 1$) were observed at large Marangoni numbers ($Ma > 10^6$). The jump increases with both decreasing subcooling and heater size.

3.2.4 Slope in SDB regime (m_{SDB})

In the SDB regime, the power law coefficient (m_{SDB} : the slope of lines 3-4 and 3'-4' in Fig. 6) for gravity effects on heat flux was found to be $m_{SDB} = 0.025$ based on aircraft data, which is significantly smaller than those in the BDB regime. However, the power law coefficient in the SDB regime had significant scatter, likely due to g-jitter in the low-G environment produced by parabolic aircraft. Since the g-jitter in the aircraft data is on the order of 0.01G, the heat transfer measured in the SDB regime is likely to be artificially high as the bubble responds to the fluctuating acceleration. In the true microgravity environment provided by the ISS, the level of g-jitter is much lower and the heat transfer can be lower as well. In fact, we hypothesize that the gravity level may not affect the heat transfer at all in the SDB regime since the shape of the bubble will not change much when the acceleration is lower than a_{tran} .

A power law coefficient of $m_{SDB} = 0$ in the SDB regime is physically reasonable. Once in the SDB regime where a non-departing, coalesced bubble covers the heater, a small change in the gravity level would only change the bubble shape without affecting the steady state value of heat transfer significantly. However, if the gravity levels continuously fluctuate, as is the case in parabolic flights where the g-jitter values are relatively large, the resulting continuous adjustments in bubble shape can induce flow around the bubble and increase the heat transfer. In essence, the g-jitter affects heat transfer more than the absolute value of acceleration in the SDB regime.

Long-duration, high-quality microgravity experiments such as MABE were needed to acquire reliable data in this regime. Indeed, the data obtained by MABE on the International Space Station in 2011 provided strong evidence that $m_{SDB} = 0$ ⁸⁾.

3.3 Experimental Validation

Based on the aircraft and MABE data, the gravity scaling parameter for pool boiling heat flux between gravity levels in the BDB and SDB regimes is given by:

$$q_{SDB}'' = q_{BDB}'' \left[\frac{a_{tran}}{a_{BDB}} \right]^{m_{BDB}} K_{jump} \quad (10)$$

where m_{BDB} , a_{tran} , and K_{jump} , are given by Eq. (5), Eq. (7), and Eq. (8), respectively.

The ability of the gravity scaling model summarized in Eq. (10) to predict the microgravity boiling data obtained on the ISS is shown on Fig. 7. The earth gravity boiling curves obtained prior to launch were used as the reference for all the prediction results. It is seen that the microgravity heat transfer can be determined quite accurately from the earth gravity heat fluxes over a wide range of subcoolings. Each subcooling includes data from three heaters sizes (7.0 x 7.0 mm², 5.6 x 5.6 mm², and 4.2 x 4.2 mm²).

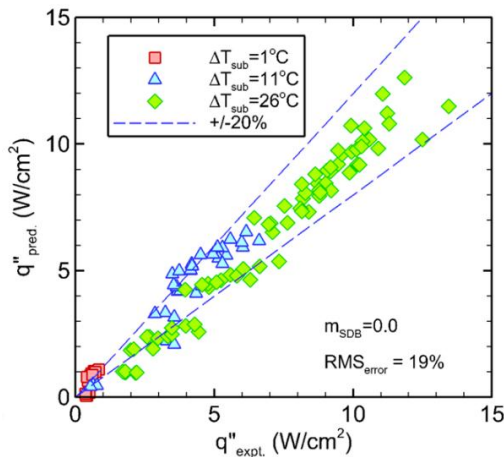


Fig. 7 Comparison of the experimental and predicted heat flux values of the ISS data using earth gravity data as the reference value.

3.4 Comparison with Other Researchers

3.4.1 Merte

Merte's group⁹⁻¹¹ studied boiling on flat heaters (19.05 x 38.1 mm²) under the long duration microgravity provided by the space shuttle (10⁻⁴G). Under these conditions, R' , the ratio of characteristic length (length of the smaller side) to the capillary length, was 0.19 and hence boiling behavior was in the SDB regime. The absence of boiling data for the entire nucleate boiling regime ruled out using the current scaling parameter to predict low-G heat fluxes. Nonetheless, some of the trends in their data agree qualitatively with the current data and can be explained by the current framework. For example, the effect of subcooling was more pronounced under low-G conditions. This was already explained in section 3.2.3 and can be attributed to increase in the jump with decreasing subcooling. Similar to the current ISS results, Merte's group also observed early onset of nucleate boiling (ONB) and heat transfer enhancement in the low heat flux regime at low-G conditions. Boiling heat transfer under low-G conditions was very small at nearly saturated conditions, similar to the observations in the current study.

3.4.2 Oka

We now discuss the trends in the data of Oka *et al.*¹²⁻¹³ wherein CHF during the parabolic flight (10⁻²G) boiling experiments were observed to follow the one-fourth power relationship while CHF during the drop tower (10⁻⁵G) experiments were significantly underpredicted using the same relationship (**Fig. 8**). For the first set of experiments¹² on the aircraft with 40x80 mm² flat heaters, CHF for CFC-113 and pentane in low-G was reduced to about 40% of the earth gravity values. A power law coefficient $m=0.25$ for CHF predicts a 32% reduction in CHF which they argued to be within the

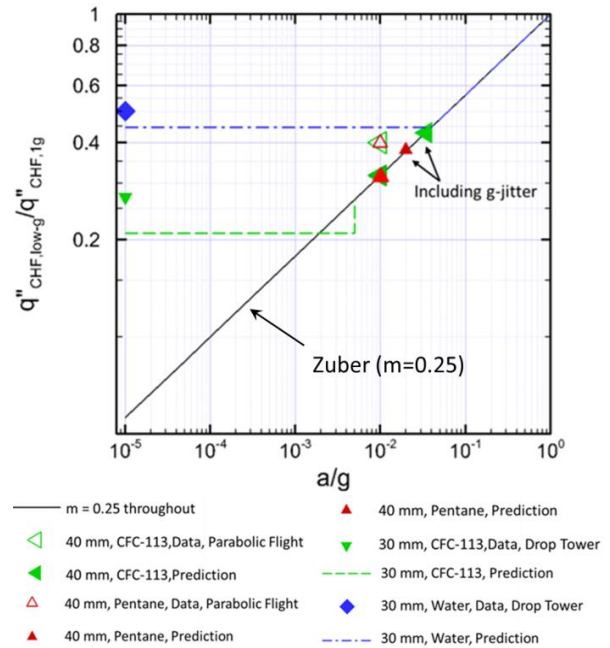


Fig. 8 Normalized CHF versus acceleration for different fluids and microgravity levels¹²⁻¹³.

experimental uncertainty limits.

Based on results of their next experiments¹³ utilizing the drop tower facility ($a/g \sim 10^{-5}$, 30x30 mm² heater), Oka doubted the validity of the one-fourth power relationship since the CHF values in these new experiments were significantly higher than those predicted by $m=0.25$ (solid line, 6% at $a/g=10^{-5}$). The current framework, however, indicates that their drop tower (10⁻⁵G) data were in the SDB regime for both water and CFC-113. Since the one-fourth power relationship is only valid in the BDB regime until transition (0.005G for CFC-113 and 0.04G for water, 30 mm heater), the current framework incorporating a jump at transition and $m=0$ in the SDB regime predicts the drop-tower CHF values for CFC-113 (dashed line) and water (dot-dashed line) very well. The relatively small between the predictions and experiments may be due to the fact that the value of C used in this example is based on FC-72 data and may not be appropriate for modeling the jump when using CFC-113 and water.

Conclusions

The effects of gravity, heater size, superheat, subcooling, and pressure and dissolved gas concentration on pool boiling heat transfer were discussed. A theoretical framework for scaling pool boiling heat flux with gravity and heater size has been validated for its robustness over a range of experimental conditions including the high-quality microgravity environment (<10⁻⁶G) available aboard the International Space Station. The

microgravity heat transfer predictions based on the modified scaling law were shown to be in excellent agreement with the experimental data. The scaling law was also able to explain previous contradictory trends in the literature.

Acknowledgement

This work was supported by NASA Grant No. NNX08AI60A through the Advanced Capabilities Division in the Exploration Systems Mission Directorate at NASA Headquarters. The authors would also like to thank ZIN Technologies and the ISS and Human Health Office at NASA Glenn Research Center in Cleveland, Ohio for fabricating the MABE test apparatus and providing support during microgravity operations, and to the European Space Agency for the opportunity to fly on the Airbus A300 Low-G aircraft.

References

- 1) W.M. Rosenhow, ASME, **74** (1952) 969.
- 2) S.S. Kutateladze: *Kotloturbostroenie*, **3** (1948) 10.
- 3) R. Raj, J. Kim and J. McQuillen: ASME Journal of Heat Transfer, **131**(9) (2009) 091502-1.
- 4) T.D. Rule and J. Kim: ASME Journal of Heat Transfer, **121**(2) (1999) 386.
- 5) R. DeLombard, J. McQuillen and D. Chao: 46th AIAA Aerospace Sciences Meeting and Exhibit, Reno, Nevada, Jan. 7 – 10, 2008.
- 6) R. Raj, J. Kim and J. McQuillen: ASME Journal of Heat Transfer, **134**(1) (2012) 011502-1.
- 7) R. Raj and J. Kim: ASME Journal of Heat Transfer, **132**(9) (2010) 091503-1.
- 8) R. Raj, J. Kim and J. McQuillen: Submitted to the ASME J. of Heat Transfer, 2012.
- 9) H.S. Lee, H. Merte, F. Chiamonte: Journal of Thermophysics and Heat Transfer, **11**(2) (1997) 216.
- 10) H.S. Lee and H. Merte: Journal of Heat Transfer, **120**(1) (1998) 174.
- 11) H.S. Lee, H. Merte and R.B. Keller: NASA/CR-1998-207410, 1998.
- 12) T. Oka, Y. Abe, K. Tanaka, Y.H. Mori and A. Nagashima: ASME Journal of Heat Transfer, **117** (1995) 408.
- 13) T. Oka, Y. Abe, K. Tanaka, Y.H. Mori and A. Nagashima: JSME International Journal, **39**(4) (1996) 798.

(Received 17 Feb. 2012)